ELSEVIER

Physica D 123 (1998) 502–512

PHYSICA D

Pulsating multiplet solutions of quintic wave equations

James M. Hyman [a,*], Philip Rosenau [b]

[a] Theoretical Division, Los Alamos National Laboratory, Los Alamos, NM 87545, USA

[b] School of Mathematical Sciences, Tel Aviv University, Tel Aviv 69978, Israel

Abstract

Numerical studies are used to demonstrate that, in addition to supporting conventional solitons, the quintic Korteweg–de Vries equation, $u_t + (u^2)_x = u_{xxxxx}$, and its regularized version, $u_t + (u^2)_x + u_{txxxx} = 0$, support multihumped solitary waves (doublets, triplets, quadruplets, etc.), referred to collectively as multiplets. Their peaks pulsate as they travel and undergo nearly elastic collisions with other multiplets. An N-humped multiplet can pulsate thousands of cycles before disassociating into an $(N-1)$-humped multiplet and a single-peak solitary wave (singlet). Although multiplets are easily created from an initial wide compact pulse, they rarely are formed by fusing singlets or multiplets in collisions. We describe the emergence and evolution of multiplets, their nearly elastic collision dynamics, and their eventual decomposition into singlets. To consider the effect of cubic dispersion on the solution of these equations, we also study $u_t + (u^2)_x + \eta u_{xxx} = \delta u_{xxxxx}$. The impact of cubic dispersion critically depends on the sign of η and its amplitude. For sufficiently large $\eta > \eta_1 > 0$, only a train of singlets emerge from an initial pulse with compact support. If η is decreased, multiplets begin to emerge leading the train of singlets. The number of humps in the multiplet increases as η is decreased, until below a critical point $\eta < \eta_\infty < 0$ the initial pulse decomposes into highly oscillatory waves. Copyright © 1998 Elsevier Science B.V.

1. Introduction

We study and compare the dynamics of multihumped solitary waves satisfying the quintic Korteweg–de Vries (qKdV) equation,

$$u_t + (u^2)_x = u_{xxxxx}, \tag{1}$$

and the quintic regularized long-wave (QRLW) equation [12],

$$u_t + (u^2)_x + u_{txxxx} = 0. \tag{2}$$

The qKdV equation has three local conservation laws,

$$u,\ u^2 \text{ and } u^3 + \tfrac{3}{2}(u_{xx})^2, \tag{3}$$

and the QRLW equation conserves

$$u,\ u^3, \text{ and } u^2 + (u_{xx})^2. \tag{4}$$

The qKdV equation is invariant under space-time stretching,

$$u \longrightarrow \beta^{-4}u, \quad t \longrightarrow \beta^5 t, \quad x \longrightarrow \beta x, \tag{5}$$

which reveals that high-amplitude patterns are narrower and propagate faster than lower-amplitude ones. In contrast, the QRLW equation is invariant under

$$u \longrightarrow \beta u, \quad t \longrightarrow t/\beta. \tag{6}$$

Thus, if $u(x,t)$ is a solution of the QRLW equation, then so is $-u(x,-t)$. Also, the amplitude affects

* Corresponding author. Tel.: +1 505 667 6294; e-mail: jh@lanl.gov.

0167-2789/98/$19.00 Copyright © 1998 Elsevier Science B.V. All rights reserved
PII S0167-2789(98)00146-8

only the timescale. In particular, the width of traveling structures of the QRLW equation is independent of the amplitude, implying there are no distinctive high-amplitude phenomena. Thus while analyzing the behavior of the QRLW equation, one can restrict both the analysis and the numerical investigations to initial data of the same amplitude. For moderate-amplitude initial data, the consequences of different scaling of the two equations are of secondary importance, and the solutions of the two equations are similar.

The observed dynamics of the qKdV and QRLW solutions are distinctly different from the solution dynamics of the cubic KdV, $u_t + (u^2)_x + u_{xxx} = 0$, or regularized long-wave (RLW), $u_t + (u^2)_x = u_{txx}$, equations. In particular, a wide variety of pulsating, multihumped, traveling solitary structures emerge from an initial wide pulse with a compact support. Both the qKdV and QRLW equations support aggregates of robust, long-persisting, coupled oscillating singlets, doublets, triplets, quadruplets, and higher-order multihumped solitary waves, which are a hybrid between conventional breathers and partially fused singlets. We refer to those multihumped structures collectively as *multiplets* and a single-humped "soliton" as a *singlet*. (Here the term soliton refers to a solitary stable structure; it does not imply integrability in the strict mathematical sense.)

1.1. Derivation of the equations

The qKdV equation can be derived via a weakly perturbative procedure which balances nonlinearity with weak dispersion. Consider the linearized dispersion relation

$$\omega = G(k) \tag{7}$$

to describe long-wave phenomena in fluids, solids, or anharmonic lattices. The typical long-wavelength (small k) dispersion relation can be expanded to

$$G(k) = a_0 k + a_1 k^3 + a_3 k^5 + \cdots \tag{8}$$

In certain complex systems, including anharmonic lattices where the lattice sites interact with their four nearest neighbors, or transmission lines with a mutual inductance (see [12] and references therein), a_1 can vanish, which, to leading order, results in the qKdV equation.

The direct truncation of the Taylor expansion, though appropriate for small k's, introduces an enormous amount of dispersion at high k's that is absent in the original process. Thus when high wave numbers are important, the solution of the qKdV equation is a questionable approximation of the solution to the original problem. This situation can be avoided by approximating $G(k)$ by a rational function that captures the behavior of $G(k)$ for large k's. Typically, $G(k)$ is bounded for all k's. This fact was taken into account in [12] and led to a derivation of the QRLW equation. The QRLW equation results from approximating (8), when $a_1 = 0$, by

$$\omega = G(k) = \frac{a_0 k}{1 + \beta k^4}. \tag{9}$$

This approximation coincides with (8) for small k's but, unlike the qKdV equation, remains bounded for large k's. In deriving the QRLW equation, the goal in [12] was not to track the details of the original dispersion but merely to avoid the ultraviolet falsetto at high k's. In this sense the QRLW equation is better suited than the qKdV to describe patterns involving higher gradients. This situation is similar to the cubic dispersive wave equations where the RLW equation is physically more realistic than the KdV at high wave numbers; however, the integrability of the KdV equation and its astounding properties have overshadowed the many advantages of the RLW equation.

Often integrable systems are considered 'superior' to the ones that are 'almost there', but lack the supporting analysis techniques that exploit the integrability. This superior outlook can prejudice the investigations of equations, such as the qKdV and QRLW, that have only a finite number of conservation laws and thus only a finite number of constraints. But the finite number of constraints may be just the freedom needed to support a wider variety of structures than those that have been observed for the KdV equation.

1.2. Traveling waves

To search for traveling waves, we substitute $s = x - \lambda t$ into the qKdV and QRLW equations. After one integration we have

$$-\lambda u + u^2 = u_{ssss} \tag{10}$$

and

$$-\lambda u + u^2 = \lambda u_{ssss}, \tag{11}$$

respectively. These equations can be brought into a universal form

$$-v + v^2 = v_{yyyy}, \tag{12}$$

where $v = \lambda^{-1}u$ and $y = \lambda^{1/4}s$ for (10) and $y = s$ for (11).

Thus while the width of the traveling structures of the qKdV equation narrow with the increase of the amplitude, the width of the traveling structures of the QRLW equation is amplitude independent. The different scaling relations of the corresponding singlets are a natural consequence of the different dispersive response of these equations at high k's (see (5) and (7)). Because for small v's, Eq. (12) implies that $v_{yyyy}+v \approx 0$, the solution and the tail of a traveling wave *will always be oscillatory.*

Eq. (12) has one integral of motion,

$$\begin{aligned} &C_0 - v^2 + \tfrac{2}{3}v^3 \\ &\quad = 2v_y v_{yyy} - (v_{yy})^2, \\ &\quad C_0 = \text{constant}, \end{aligned} \tag{13}$$

and can be reduced to second order by defining $G = (\mathrm{d}v/\mathrm{d}y)^{3/2}$;

$$C_0 - v^2 + \tfrac{2}{3}v^3 = \tfrac{4}{3}G^{5/3}G_{vv}, \tag{14}$$

but no further reduction seems possible. The analysis is even more complex for the pulsating multiplets. Although we can create multiplets easily from any compact initial data with appropriate width and/or amplitude, we have been unable to explicitly solve for any of these structures.

2. Numerical experiments

Our investigation of the emergence and stability of the multiplets is primarily computational, and we have little analytical handle on the 'how and why' for the creation and dynamics of the multiplets.

In our calculations, we approximated the spatial derivatives with a pseudospectral method using the discrete Fourier transform (DFT). The equations were integrated in time with a variable-order, variable-timestep Adams–Bashford–Moulton method. The numerical errors were monitored by varying the number of discrete Fourier modes between 128 and 512 and varying the estimated time error per unit step between 10^{-6} and 10^{-9} to ensure that the solutions were well converged. Most of the calculations shown here solved the conservative form of the equations with 256 DFT modes, a time error of 10^{-8} per unit time.

To reduce the errors due to aliasing, we filtered the time derivatives by explicitly adding an artificial dissipation term to the equations. This term was defined in Fourier space to approximate the effects of linear second-order dissipation $\Delta x u_{xx}$ on the top $\frac{1}{3}$ of the Fourier modes, have no effect on the lower $\frac{1}{3}$ of the modes, and have a linear transition between the two regions. To identify numerical artifacts due to aliasing and other discrete effects, we compared the solutions of the equations when they were differenced in conservation and nonconservation form.

Most of the examples in this section use initial data with compact support of the form

$$u(x, t = 0) = \begin{cases} A\cos^2(Bx - C) & \text{if } |Bx - C| \le \dfrac{\pi}{4}, \\ 0 & \text{otherwise}, \end{cases} \tag{15}$$

where A, B, and C are constants.

After illustrating the dynamics of the multiplet solutions of the qKdV equation, we will compare these solutions with those of the QRLW equation. Finally, we will show how cubic dispersion alters the structure of the emerging multiplets.

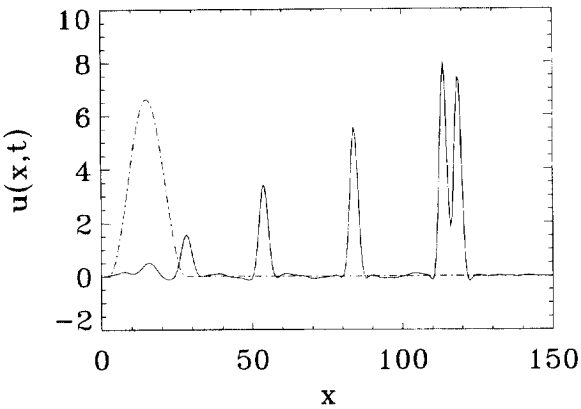

Fig. 1. The initial conditions (15), $A = 20/3$, $B = 1/4$, and $C = 25/4$ (illustrated by a dash–dot line), for the qKdV equation decompose into a train of singlets and a single doublet by time $t = 15$ (illustrated by a solid line). The doublet is traveling with speed approximately 6.52.

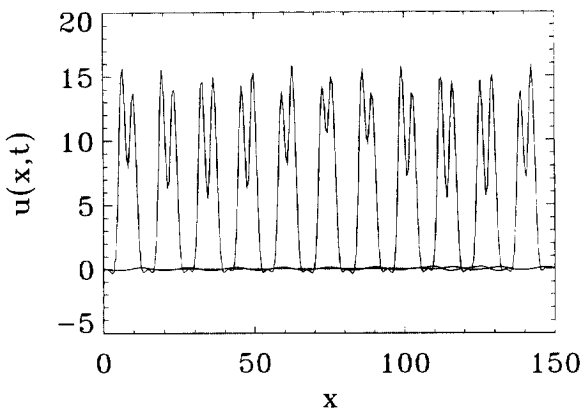

Fig. 2. The strongly bound doublet is shown at times $t = 0, 1, 2, \ldots$ in a domain with periodic boundary conditions. This calculation was continued until the doublet had traveled a distance of over 4000 and still retained approximately the same height and speed.

2.1. The qKdV equation

In Fig. 1, we observe an initial pulse for the qKdV equation (1) desolving into a train of solitary waves led by a doublet. *Without exception, in all numerical simulations the multiplet structure emerges at the front.* Notice the dip in front of the singlets and the oscillatory tails. In Fig. 2, the doublet initial data evolve under the qKdV equation in a periodic domain and are shown at times $t = 0, 1, 2, \ldots$ This calculation was continued

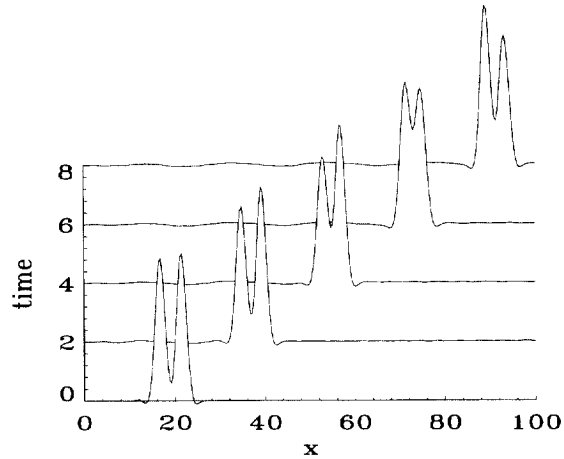

Fig. 3. A weakly bound double, traveling initially at speed 9, is shown at times $t = 0, 2, 4, \ldots$ satisfying the qKdV equation.

beyond $t = 300$ at which time the doublet was still tightly bound together. Observe the pulsating peaks and the undulating valley between them. When the forward pulse is higher, it travels faster and the doublet widens; when the trailing pulse is higher, it travels faster and tries to override the leading pulse, causing the structure to narrow. These oscillations modulate the speed and width of the doublet so that it resembles a traveling breather.

In Fig. 3 a weakly bound doublet slowly sheds energy into the tail (visible behind the doublet at $t = 8$) on each pulsation. The strength of the bound state is related to how close the valley between the states approaches zero on each pulsation. The valley in this doublet is closer to zero than in the strongly bound doublet in Fig. 1. The radiation loss causes a slow decrease in amplitude and a continuous deepening of the valley until, at $t \approx 79$, the valley almost touches zero and the doublet decomposes into two solitary waves. When a doublet decomposes, the lead singlet must be the faster (taller) one, running away from its sibling.

Using the qKdV symmetry (5) with $\beta = -1$, we can reverse the decomposition process in Fig. 4 to create initial data that will fuse into a doublet. That is by defining $u_0(x) = u(-x, t = 85)$ as initial data for the qKdV equation, the two singlets will fuse at time $t = 10$. We did this, and observed that the states remained bound until about $t = 200$, when they again

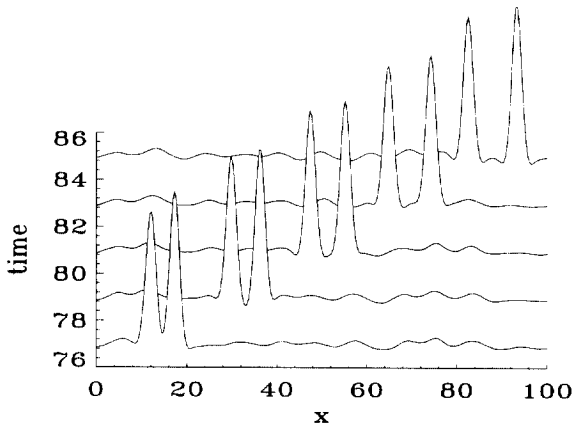

Fig. 4. The doublet shown in a, shown at times $t = 76, 78, 80, \ldots$, decomposes into to singlets traveling at speeds approximately 8.6 and 9.5.

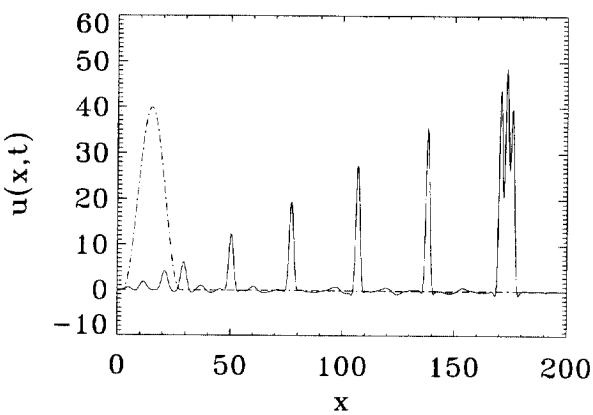

Fig. 5. The initial conditions in Fig. 1 were amplified by a factor of 4, (15) $A = 80/3$, $B = 1/4$, and $C = 15/4$. The solution of the qKdV equation decomposes into a train of singlets and a triplet by time $t = 4$ (the solid line).

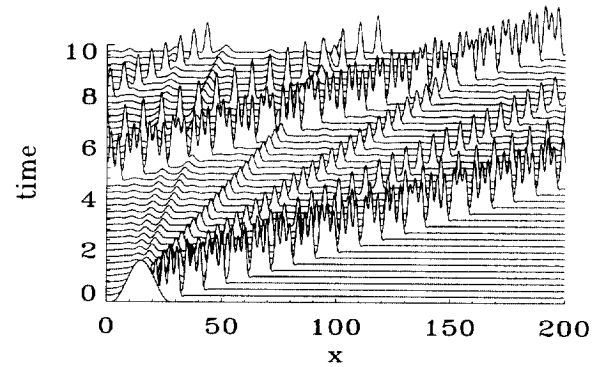

Fig. 6. The space–time evolution of the initial conditions shown in Fig. 5 in a domain with periodic boundary conditions. Notice how the triplet remains intact after several collisions with the other singlets. Also, the phase shift of the two slowest singlets, after a collision with the triplet at $t = 5$, can be observed.

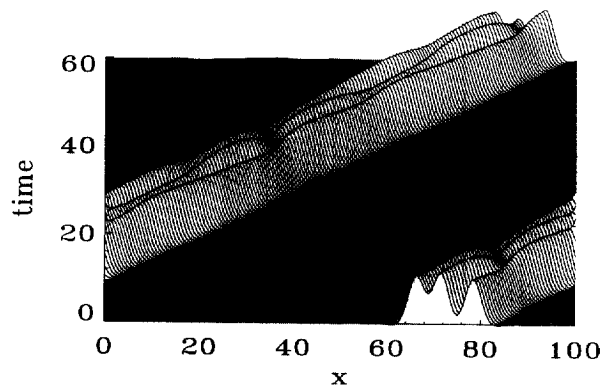

Fig. 7. Space–time surface plot for the evolution of a triplet for the qKdV equation. Note how the three bound peaks pulsate up and down as they travel through space.

separated. We never observed two singlets fusing into a doublet unless the initial data were defined in this special manner. We ran numerical experiments where two singlets with nearly equal velocity collided, where three singlets collided simultaneously, and where a singlet collides slowly with a doublet or higher-order multiplet. The collision to fuse singlets or multiplets together seems to require the oscillating peaks or tails be in 'phase'. Without explicit understanding of the process, we were only able to fuse singlets or multiplets by propagating a multiplet until it decomposed, and then using the space–time symmetry to define initial conditions that were equivalent to propagating the multiplets back in time so they were again bound states.

The initial conditions for the qKdV equation in Fig. 5 are four times higher than those in Fig. 1. The higher initial conditions result in creating a train of solitary waves with a triplet, instead of the doublet observed in Fig. 1, leading the pack. The robust stability of the triplet is shown Figs. 6 and 7, where the triplet remains tightly bound after several collisions. If the initial pulse is made wider, a triplet may still emerge from the initial data, even when the pulse is reduced

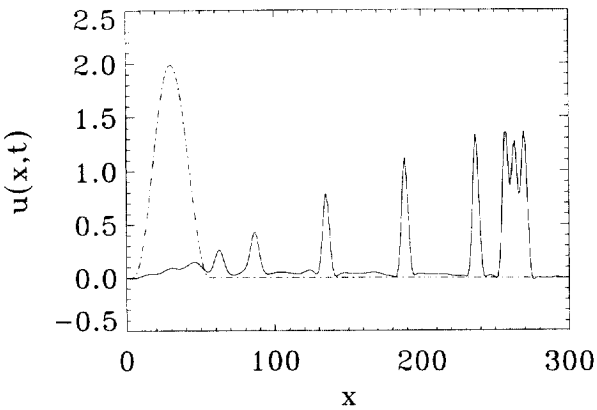

Fig. 8. Initial conditions in Fig. 1 were decreased in height by a factor of one-third and widened by a factor of 2, (15) $A = 80/9$, $B = 1/8$, and $C = 15/8$. Again the initial pulse decomposed into several singlets and a triplet, shown at $t = 150$ by the solid line. The triplet is traveling with velocity approximately equal to 1.3.

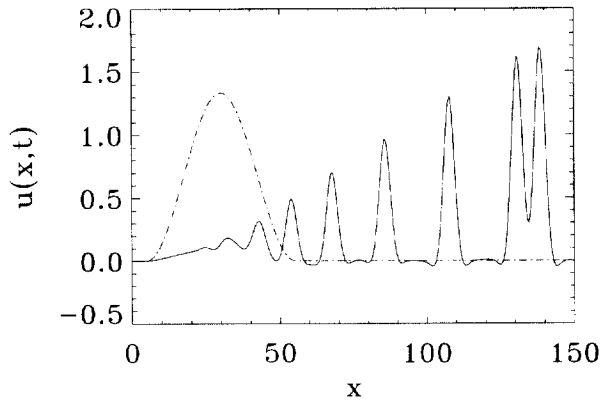

Fig. 9. The initial conditions (15), $A = 7/4$, $B = 1/7$, and $C = 20/7$ (illustrated by a dash–dot line) for the QRLW equation decompose into a train of singlets and a single doublet (illustrated by a solid line) at time $t = 75$. The doublet is traveling with velocity approximately equal to 1.36.

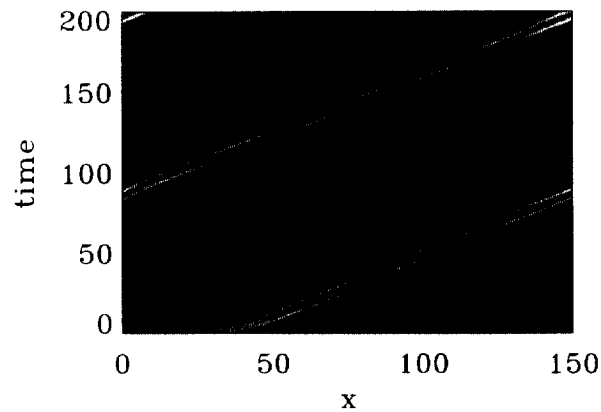

Fig. 10. The lighter shades in the density plot indicate larger-amplitude values in this shaded space–time plot of the solution in Fig. 9.

in amplitude as in Fig. 8. As the pulse is made even wider (or higher, because of the scaling (5) between changes in height and width), the number of humps in the leading multiplet increases to become a quadruplet, quintuplet, or higher-order multiplet.

2.2. The QRLW equation

We observed behavior in our numerical experiments for the QRLW equation similar to that just described for the qKdV equation. The scaling (6) implies that changes in the amplitude of the solution will only alter the time scale of the evolution and not the trajectory or shape of the solution such as the number of humps in the emerging multiplet. Changes in the width of the initial conditions do affect the resulting pattern.

In Fig. 9 we observe an initial pulse for the QRLW equation breaking into a train of singlets and a leading doublet. Note the similarity between this solution and the qKdV solution in Fig. 1. The further evolution of the solution and the collision dynamics is displayed in the space–time diagram in Fig. 10. Notice that both the width and height of the doublet pulsate and that there is a phase shift in the slower singlets after they collide with the faster multiplet at time $t = 125$ and $t = 150$.

In Fig. 11 the collision of a doublet with a slower, weakly bound doublet breaks the slower doublet into two singlets. In numerical experiments with strongly bound doublets, the doublets have been observed to survive hundreds of collisions and remained intact.

Because of the symmetry (6) for the QRLW equation, a negative pulse will travel to the left. Fig. 12 shows the robustness of a right traveling doublet colliding with a left traveling negative singlet. In this and other numerical experiments, these collisions are observed to be as robust as the collision between the positive multiplets and singlets. The collision is slightly

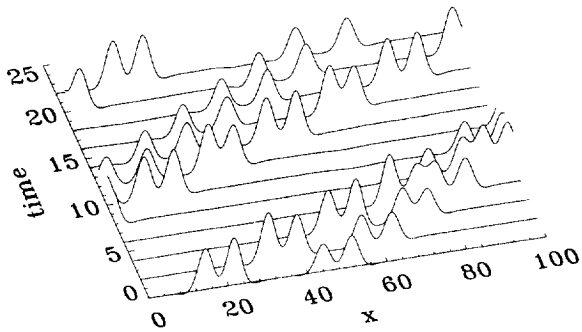

Fig. 11. Initially, the doublet centered at $x = 20$ is traveling faster than the weakly bound doublet at $x = 50$ and overtakes it at $t = 5$. After the collision, the slower doublet decomposes into two singlets.

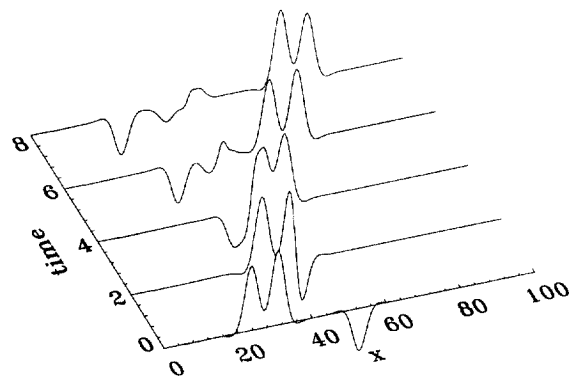

Fig. 12. A negative singlet for the QRLW traveling to the left remains intact after colliding with a doublet traveling to the right. Note the ripple left at the location of the collision.

inelastic and leaves a small 'ripple' behind at the collision site.

In Fig. 13 the evolution of a 9-plet is shown. The solution was generated with a square wave initial condition that quickly transitions into the 9-plet. By the same method, one can create multiplets with an arbitrary number of peaks.

The initial pulse in Fig. 9 was made wider in Fig. 14 and decomposes into a train of singlets lead by a triplet. The space–time plots in Fig. 15 follow the evolution of this pulse until at $t \approx 475$ the triplet decomposes into a doublet and a singlet. The lines representing the triplet start to separate at about $t = 450$ in Fig. 16. Also note the oscillations between the triplet bound states, the robustness of the collisions, and the

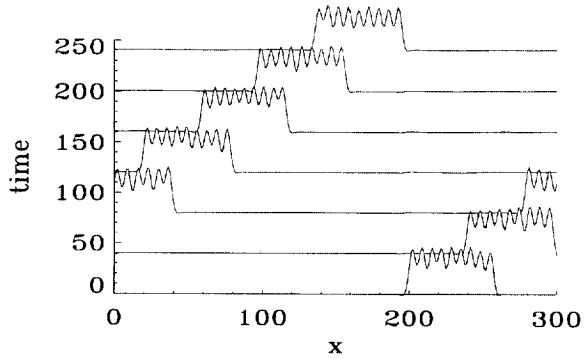

Fig. 13. A QRLW 9-plet solitary wave was created by evolving an initial square wave pulse. Shown here at later times, the peaks pulsate up and down as it propagates.

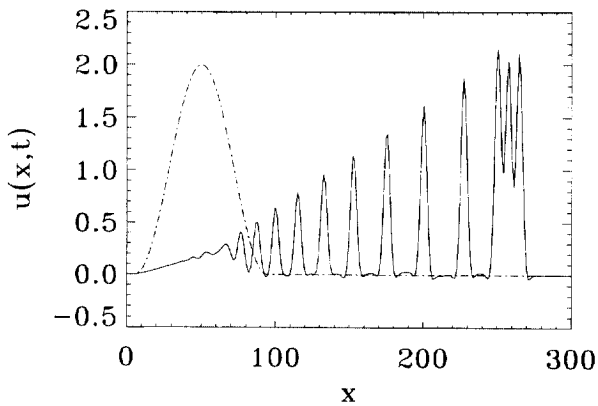

Fig. 14. The initial pulse (15), $A = 2$, $B = 1/28$, and $C = 50/28$, is wider than in Fig. 10 and decomposes into a train of singlets and a triplet. This figure follows the evolution of this triplet until it breaks up at time $t \approx 475$.

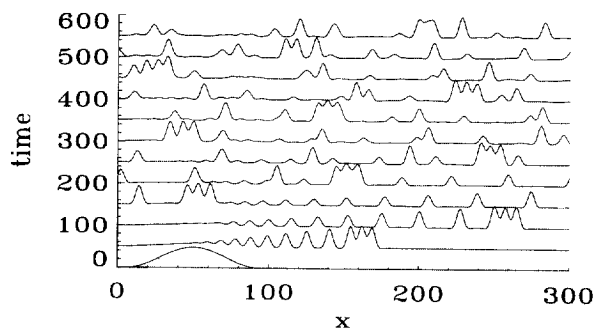

Fig. 15. The space–time plot of the solution for the QRLW equation shown in Fig. 14. The initial conditions decompose into a train of singlets and a triplet; the triplet eventually decomposes at $t \approx 475$.

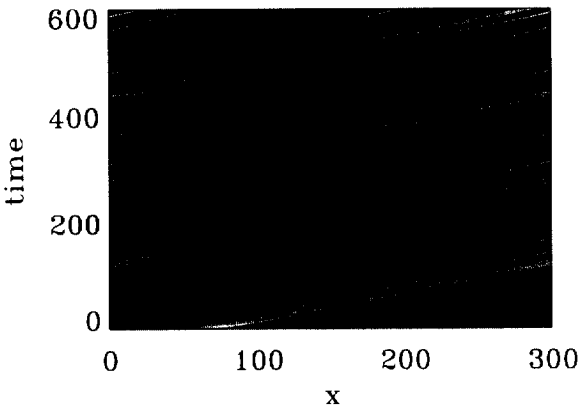

Fig. 16. The space–time density plot of the solution shown in Fig. 15.

phase shift when the triplet collides with the slower traveling singlets. All collisions we observed were remarkably robust, even though they were slightly inelastic and energy was lost to the medium.

3. The effects of cubic dispersion

In most of the previous investigations of the cubic–quintic KdV (cqKdV) equation

$$u_t + (u^2)_x + \eta u_{xxx} = \delta u_{xxxxx}, \tag{16}$$

(cf. [1–11,13]), the cubic dispersion is assumed to be the dominant mechanism. Note that in the quintic KdV equation appropiate for water waves, the quintic dispersion has opposite sign, $\delta < 0$, than in the qKdV equation (16). This difference can be easily reconciled by the transformation

$$u \longrightarrow -u, \quad t \longrightarrow -t, \quad \eta \longrightarrow -\eta, \tag{17}$$

which changes the sign of δ (but also switches the sign of the solution). Indeed, the numerical experiments presented for $\delta < 0$ in [10] use negative initial data and the resulting waves travel to the left, as expected. This case is modeled via the cqKdV equation using positive initial data, and $\eta < 0$.

Eq. (17) reduces to the qKdV equation when $\eta = 0$ and $\delta > 0$ and (after appropriate scaling) to the KdV equation as $\eta \to \infty$. Most of the theoretical studies of (16) have been confined to small δ, when the cqKdV equation can be treated as a perturbation of the KdV (which enables its integrability to be exploited). The integrability of the KdV equation is like a lantern attracting the dynamics of nearby nonintegrable systems and their practitioners. It so happens that the multiplets hide in the shadow zone beyond the light of integrability.

In the absence of cubic dispersion ($\eta = 0$), Eq. (16) can no longer be treated as a perturbation of the KdV equation. Eliminating the cubic dispersion increases the chances of determining if quintic dispersion generates a different phenomenology than the classic soliton dynamics of the KdV equation. By focusing on the role of the quintic dispersion in the creation of the multiplets, it became clear that the cubic dispersion undermines their stability. Stable multiplets were only observed when δ was above a certain finite threshold, depending on the amplitude of the multiplet.

Previous attempts based on asymptotic analyses have been used to construct steady traveling waves with two or three humps and oscillatory structures sampling both positive and negative values (cf. [4]). These multihumped structures were also constructed numerically in [10], but as their evolution reveals [9], they are structurally unstable and decompose into singlets. In the hundreds of numerical experiments we have performed on these equations, all the multiplets pulsated both in height, width, and velocity (cf. Figs. 1 and 7). Thus the speed of each hump in a multiplet is not constant, but modulates around a constant. Such structures cannot be simply composed out of solitons traveling with the same speed.

3.1. Nonnegative cubic dispersion

The number of humps of the multiplets is perhaps is the most interesting aspect of solution of the cqKdV equation. For the initial data (15) ($A = 2$, $B = 1/28$, $C = 5 - /28$), only singlets emerge for $\eta > 1.5 = \eta_1$. This result is illustrated in Fig. 18 ($\eta = 1.5$), where the solution is shown at $t = 0$ by the dash–dot line and at time $t = 100$ by the solid line. As the cubic dispersion is reduced, first doublets appear ($\eta = 1$, Fig. 18), followed

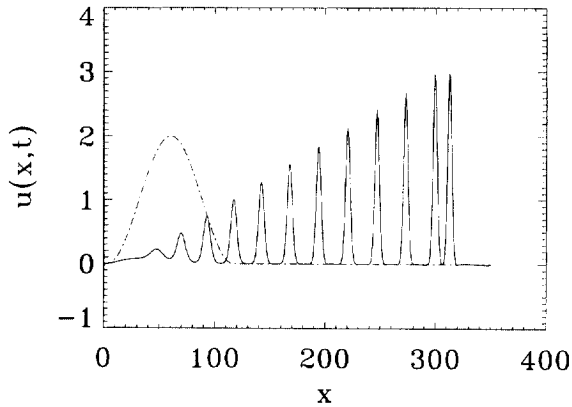

Fig. 17. $u_t + (u^2)_x + \frac{3}{2}u_{xxx} - u_{xxxxx} = 0$. For large cubic dispersion, only singlets emerge from the initial pulse.

by triplets, quadruplets ($\eta = 0.5$, Fig. 19), and quintuplets ($\eta = 0$, Fig. 20) for the qKdV equation. There does not appear to be a critical transition when η crosses zero, and the leading multiplet continues to gain humps for negative η ($\eta = -1$, Fig. 21). At a point just below $\eta = -2$, there is a dramatic change in the decomposition of the initial pulse, and it decomposes into a highly oscillatory wave instead of a multiplet followed by a train of singlets.

In Figs. 17–21, note how as η decreases, not only do the number of peaks in the emerging multiplet increase, but the singlets become narrower and the valleys between them widen and become more oscillatory. At first, these oscillations are almost

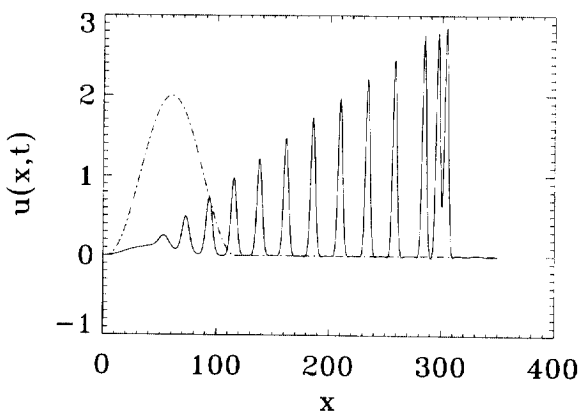

Fig. 18. $u_t + (u^2)_x + u_{xxx} - u_{xxxxx} = 0$. As the cubic dispersion decreases, a doublet emerges leading a train of singlets.

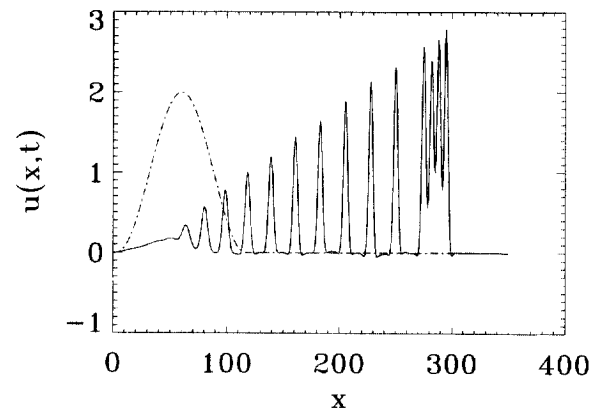

Fig. 19. $u_t + (u^2)_x + \frac{1}{2}u_{xxx} - u_{xxxxx} = 0$. As the cubic dispersion is further reduced, the leading multiplet becomes a quadruplet.

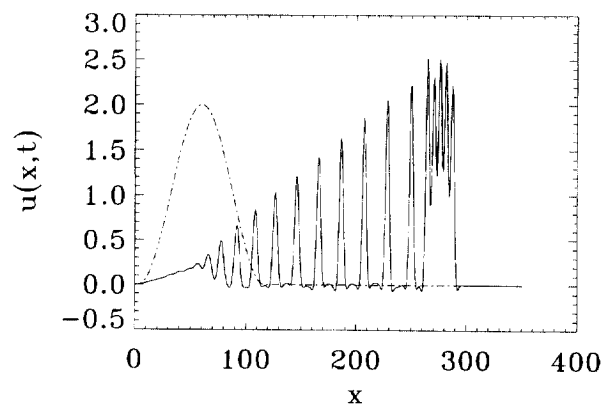

Fig. 20. $u_t + (u^2)_x - u_{xxxxx} = 0$. When there is no cubic dispersion, the leading multiplet solution of the qKdV equation has five humps.

unnoticeable, but ultimately they win out and for $\eta < \eta_\infty \approx -2$ the initial pulse decomposes into large-amplitude oscillations that fill the domain.

The same trend is observed for other initial data, but with different transition values for η. For example, if the initial data are wider (or taller), the leading multiplet has more humps. This is illustrated for $\eta = 1.5$ by the emerging triplet in Fig. 22, where the initial data are twice as tall as those in Fig. 17 where only singlets emerge from the initial data.

It appears to be a general property that for every initial pulse where an N-plet emerges, there are associated bounds such that, as long as $\eta_N < \eta < \eta_{N-1}$,

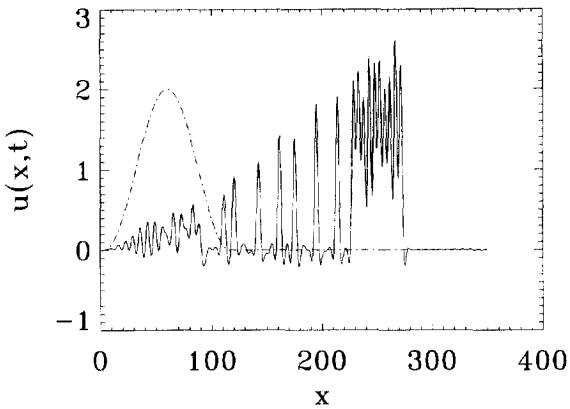

Fig. 21. $u_t + (u^2)_x - u_{xxx} - u_{xxxxx} = 0$. For negative cubic dispersion, the number of humps continues to increase as the dispersion is reduced.

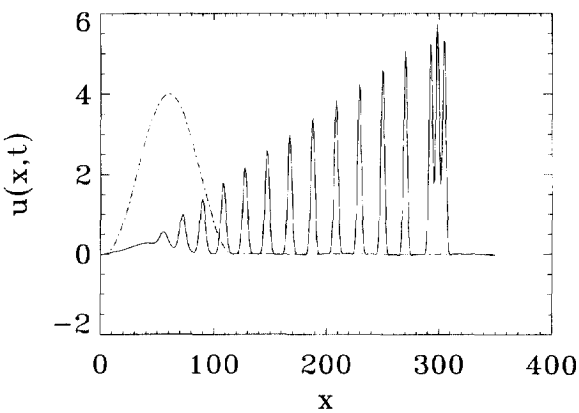

Fig. 22. $u_t + (u^2)_x + \frac{3}{2}u_{xxx} - u_{xxxxx} = 0$. When the initial conditions in Fig. 17 are made twice as tall, instead of only singlets emerging, the leading multiplet is a triplet.

the emerging multiplet has N humps. If $\eta > \eta_{N-1}$, the number of humps decreases by one. As η is further increased, then the number humps continues to decrease until $\eta > \eta_1$, when only singlets are seen to emerge.

Thus all changes in the number of emerging multiplets are confined to the $[\eta_\infty, \eta_1]$ interval. Recall, however, that an emerging N-plet decomposes after a while into an $(N-1)$-plet and a singlet, and though different initial data may initially beget multiplets with the same number of humps, these multiplets are not identical and usually will differ from each other in their detailed structure (most notably the width of their valleys). Therefore, the time at which the emerging multiplets decompose does depend upon η. In numerical experiments, we have observed that if η is only slightly smaller than η_{N-1}, the emerging N-plet will decompose into an $(N-1)$-plet and a singlet much sooner than if η is smaller and closer to η_N.

For fixed values of δ and η, there may be multiplets with different numbers of humps and multiplets with the same number of humps, but very different behavior. Because the multiplets slowly shed energy to the background and lose their humps one by one, the values of δ and η that support an N-plet will also support multiplets with a smaller number of humps and the same amplitude. Also, as the multiplets lose their energy, they are bound less strongly. Thus, there can be both strongly bound multiplets that persist for very long times and weakly bound multiplets that quickly decompose.

Next we investigate the effect of fixing $\eta = 1$ and varying δ. In the KdV limit ($\delta = 0$), Fig. 23 shows the initial data for Eq. (16) breaking into a train of classic KdV solitons. As δ decreases, first a doublet emerges ($\delta = -0.5$, Fig. 24) followed by a train of singlets that are qualitatively similar to those of the KdV equation. Also, note that as δ decreases, the spacing between the emerging singlets increases, there are fewer singlets, and their amplitudes slightly increase. As expected, for a doublet to appear, δ has to be above a threshold dependent upon the shape of the initial

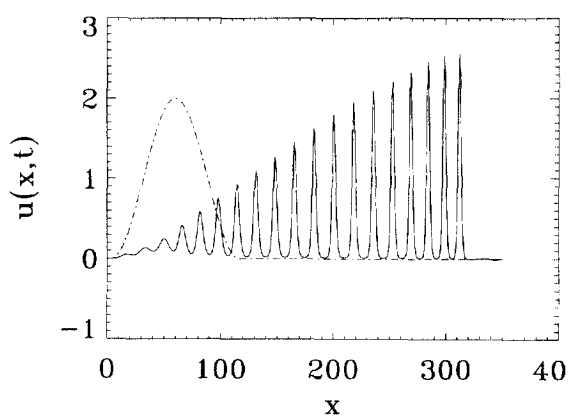

Fig. 23. $u_t + (u^2)_x + u_{xxx} = 0$. The solution of the KdV equation decomposes into classic solitons.

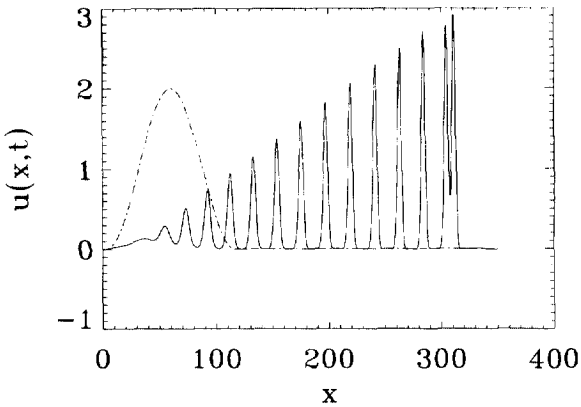

Fig. 24. $u_t + (u^2)_x + u_{xxx} - \frac{1}{2}u_{xxxxx} = 0$. When quintic dispersion is added to the KdV equation, a doublet emerges at the head of the train of singlets.

pulse. Decreasing the quintic dispersion further results in the leading multiplet having more and more humps.

3.2. Negative cubic dispersion

Though most of our studies were devoted to positive cubic dispersion with $\eta > 0$ and $\delta > 0$, in modeling water waves, negative dispersion is appropriate. The linearized dispersion equation

$$\omega = \delta k^5 + \eta k^3 \tag{18}$$

for the cqKdV equation (16) illustrates the competition between the quintic and cubic dispersions when $\delta\eta < 0$. Indeed, for $\eta < 0$, the cubic dispersion destabilizes solitary waves, and if $-\eta$ is large enough, the cubic dispersion prevents the formation of stable multiplets. Note that just as for the positive case, when η is small, its impact is secondary and multiplets are commonly observed. Previously, negative doublets were observed in the numerical experiments of (16) with $\delta < 0$ and $\eta > 0$ [10]. These simulations can be transformed into positive doublet solutions of Eq. (16) exactly in the range of small negative η. After rescaling the equation in [10] to (16), the transformed coefficients are $\delta = 1$ and $\eta = -1/\sqrt{40}$.

Acknowledgements

This research was supported by the US Department of Energy under contracts W-7405-ENG-36 and KC-07-01-01. The work of Philip Rosenau was supported in part by the BSF grant no. 94-00283.

References

[1] J.P. Boyd, Numerical computations of a nearly singular nonlinear equation: weakly nonlocal bound states of solitons for the fifth-order Korteweg–de Vries equation, J. Comput. Phys. 124 (1) (1996) 55–70.
[2] D.C. Calvo, T.R. Akylas, On the formation of bound states by interacting nonlocal solitary waves, Physica D, sub judice.
[3] B. Dey, A. Khare, C. Kumar, Stationary solitons of the fifth-order KdV-type, equations and their stabilization, Phys. Lett. A 223 (6) (1996) 449–452.
[4] R. Grimshaw, B. Malomed, E. Benilov, Solitary waves with damped oscillatory tails: an analysis of the fifth-order Korteweg–de Vries equation, Physica D 77 (4) (1994) 473–485.
[5] J.K. Hunter, J. Scheurle, Existence of perturbed solitary wave solutions to a model equation for water waves, Physica D 32 (2) (1988) 253–268.
[6] K. Kano, T. Nakayama, An exact solution of the wave equation $u_t + uu_x - u_{(5x)} = 0$, J. Phys. Soc. Jpn. 50 (2) (1981) 361–362.
[7] V.I. Karpman, Radiation by solitons due to higher-order dispersion, Phys. Rev. E (3) 47 (3) (1993) 2073–2082.
[8] V.I. Karpman, Stationary solitary waves of the fifth-order KdV-type equations, Phys. Lett. A 186 (4) (1994) 300–302.
[9] S. Kichenassamy, P.J. Olver, Existence and nonexistence of solitary wave solutions to higher-order model evolution equations, SIAM J. Math. Anal. 23 (5) (1992) 1141–1166.
[10] B. Malomed, J.M. Vanden-Broeck, Solitary wave interactions for the fifth-order KdV equation, Mathematical Problems in the Theory of Water Waves, Luminy, 1995, Contemp. Math., vol. 200, Amer. Math. Soc., Providence, RI, 1996, pp. 133–143.
[11] H. Nagashima, M. Kuwahara, Computer simulation of solitary waves of the nonlinear wave equation $u_t + uu_x - \gamma^2 u_{5x} = 0$, J. Phys. Soc. Jpn. 50 (11) (1981) 3792–3800.
[12] P. Rosenau, Dynamics of dense discrete lattices – High-Order effects, Prog. Theor. Phys. 79 (1988) 1028.
[13] Y. Yamamoto, E.I. Takizawa, On a Solution on nonlinear time-evolution equation of fifth-order, J. Phys. Soc. Jpn. 50 (5) (1981) 1421–1422.